

Competing role of Interactions in Synchronization of Exciton-Polariton Condensates

S. Khan and H. E. Türeci

Department of Electrical Engineering, Princeton University, Princeton, New Jersey 08544, USA

(Dated: October 14, 2016)

We present a theoretical study of synchronization dynamics in incoherently pumped exciton-polariton condensates in coupled traps, based on an expansion in non-Hermitian modes appropriate for the pumped system. We find that polariton-polariton and reservoir-polariton interactions play competing roles and lead to qualitatively different synchronized phases as pumping power is increased. Crucially, these interactions can also act against each other to hinder synchronization. We present a phase diagram and discuss the general characteristics of these phases using a generalized Adler equation.

Synchronization is a ubiquitous phenomenon in dynamical oscillating systems[1] that has recently seen renewed interest across diverse setups, from electro/opto-mechanical oscillators [2–5], to lasers [6–8], trapped atoms [9–11], and many-oscillator arrays [12–14], while quantum effects have also been explored [15–18]. However, a description of synchronization in strongly nonlinear, driven-dissipative exciton-polariton systems has yet to be fully discussed. In these systems, synchronization appears as the natural mechanism to explain [19] the formation of spatially extended condensates across disorder-generated localized photonic traps, prevalent in early experiments [20]. It was later pointed out [21] that synchronization can also take place between extended modes that overlap. While such effects are present in photon lasers as well [22–24], what distinguishes polariton condensates are strong nonlinear interactions. One may then ask whether these interactions can give rise to *qualitatively* different synchronization physics in polariton condensates. Our present work answers this question: we show that interactions in polaritonic systems lead to two competing effects, which not only lead to characteristically different synchronized phases, but can also actively prevent the emergence of synchronization.

Fundamentally, we study the synchronization of two coupled oscillators; however, the unique platform of exciton-polariton condensates under incoherent pumping modifies this picture significantly. In these incoherently pumped systems, an uncondensed fraction of polaritons (the “reservoir”) is deposited by the pump typically at high energies. Interactions amongst them give rise to stimulated scattering towards lower energy states, which can then undergo an instability and condense at a threshold pump strength P_1^L . The condensate mode above this threshold power appears with a self-organized frequency and associated spatial pattern. In a typical scenario, above a second threshold P_2^L , a second mode condenses with generally a different oscillation frequency. While such threshold physics is similar to the photon laser, exciton-polaritons distinguish themselves with strong, pump-dependent nonlinear interactions, which come in two varieties. Quasi-particles belonging to the condensate interact, giving rise to purely energetic effects. On the other hand, the deposited reservoir polaritons provide both a repulsive potential and the source of gain that allows condensation in the first place. Both interactions can significantly modify the two oscillation frequencies above the second threshold to eventually lock the two oscillators to a single

frequency at the synchronization threshold. Crucially, these interactions strongly depend on quasi-particle density and hence pump power. This leads to an effective *pump-dependent* interaction between the oscillators that is different from Huygens’ original clock oscillator model of synchronization [25, 26].

As we will also show, the strong interactions in polariton condensates mediate frequency modulation that can cause detuned modes to synchronize; this is different from the photon laser, where relatively weaker interactions fail to lower the threshold for synchronization below that of other instabilities (e.g. a third mode turning on), except under very special conditions (very small modal detuning and large spatial overlap, enhanced e.g. in resonators that have a quasi-degeneracy [27]). Overall, the simple picture of two coupled oscillators is significantly enriched by the presence of threshold physics, pump-dependence, reservoir dynamics, and interactions. Our work aims to capture these rich dynamical features by employing a temporal coupled mode theory (TCMT) based on a modal description of condensate dynamics introduced in our recent work [28]. This description allows us to develop an analytical model based on a multivariable generalized Adler equation, and to draw conclusions for the long-time limit of the dynamics for a wide parameter regime. Our key result is a phase diagram which reveals the presence of distinct synchronized phases when either of the two interactions is dominant, and a desynchronized phase when both interactions are actively competing.

Model - We study the interaction of condensate modes in two tunnel-coupled and detuned polariton traps with a trapping potential $\mathcal{V}(\mathbf{r})$, under a uniform incoherent pump with pump strength P and spatial profile $f(\mathbf{r})$ [See Fig. 1 (a)]. Such models have been realized with coupled micropillars to study self-trapping of polaritons [29, 30]. Condensate dynamics under incoherent pumping can be described by the generalized Gross-Pitaevskii equation (gGPE) for the order parameter $\Psi(\mathbf{r}, t)$ (we set $\hbar = 1$):

$$\begin{aligned} i\partial_t \Psi &= \left[-\frac{\nabla^2}{2m} + \mathcal{V}(\mathbf{r}) + \left(g_R + i\frac{R}{2} \right) n_R + g|\Psi|^2 - i\frac{\gamma_c}{2} \right] \Psi \\ \partial_t n_R &= Pf(\mathbf{r}) - \gamma_R n_R - Rn_R |\Psi|^2 \end{aligned} \quad (1)$$

The pump generated reservoir of excitons (density n_R , loss γ_R) acts as a source of gain $\propto R$ leading to the formation of a coherent condensate when polariton losses γ_c are overcome. In addition, two distinct types of interparticle interactions are

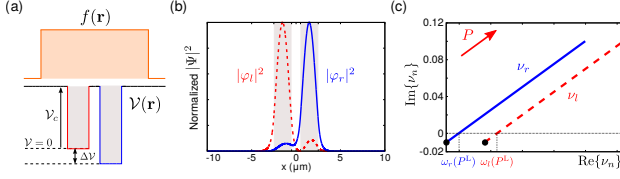


FIG. 1. (a) Trapping geometry $V(r)$ and pump profile $f(r)$. (b) Probability density of the two non-Hermitian pump modes used to project the gGPE. (c) Evolution of the associated complex-valued eigenvalues $\nu_n(P)$ with pump power in the ω - γ plane.

active: between polaritons within the condensate (strength g), and between reservoir excitons and condensate polaritons (strength g_R).

The temporal coupled-mode theory (TCMT) for the gGPE [28] projects the condensate amplitude $\Psi(\mathbf{r}, t)$ and the reservoir density $n_R(\mathbf{r}, t)$ onto a set of well-defined non-Hermitian *pump modes* that account for the pumped and dissipative trapping potential. Generally, there is a pumping range wherein it is sufficiently accurate to truncate the projection to only two modes. We consider specifically a detuned trap regime here, where the two modes are predominantly confined to the left or right trap; these modes are denoted by φ_l and φ_r respectively, and shown in Fig. 1 (b). We emphasize that these pump modes are *not* simply eigenmodes of the individual traps; rather they account for tunneling between the traps, the unsaturated pump, and dissipation through cavity loss [28]. Their associated complex pump-dependent eigenvalues $\nu_n(P) = \omega_n(P) + i\gamma_n(P)$, $n = l, r$ therefore describe pump-induced dynamics in the *linear* modal theory. The real part $\omega_n(P)$ defines the mode frequency which evolves with P due to the pump-induced blueshift, while the imaginary part $\gamma_n(P)$ represents the net gain, a balance between pump-induced amplification and polariton loss. In the absence of pump-induced repulsion, the modal frequencies are ω_{l0} and ω_{r0} , determined by the trapping potential alone; we choose $\omega_{l0} > \omega_{r0}$, and define the pump mode detuning $\Delta\omega \equiv \omega_{l0} - \omega_{r0}$. The use of a wide, homogeneous pump spot simplifies the pump's influence: both modes experience an equal blueshift and similar gain from the pump-generated reservoir, as is evident from the evolution of mode eigenvalues with P , shown in Fig. 1 (c).

These pump modes are then used to expand the full condensate wavefunction $\Psi = \sum_{n=l,r} a_n(t)\varphi_n$, and then to project Eqs. (1). This leads to the TCMT with nonlinear interactions and pump depletion - a set of dynamical equations for the amplitudes $a_n(t)$ and reservoir matrix elements $N_{nm}(t) = \int d\mathbf{r} \varphi_n \varphi_m [n_R - \frac{1}{\gamma_R} P f(\mathbf{r})]$ that describe the change in the reservoir density as measured from its unsaturated value [31]. These dynamical equations for $\{a_n(t), N_{nm}(t)\}$ can be recast into a more useful form by first expressing the mode coefficients in amplitude and phase variables, $a_n(t) = \bar{a}_n(t)e^{-i\phi_n(t)}$, and then rewriting the mode

equations in terms of the dynamical variables $\{\phi, z, \rho\}$, where:

$$\phi = \phi_l - \phi_r, \quad z = \frac{\bar{a}_l^2 - \bar{a}_r^2}{\bar{a}_l^2 + \bar{a}_r^2}, \quad \rho = \bar{a}_l^2 + \bar{a}_r^2 \quad (2)$$

Here ϕ is the relative phase, z the normalized modal intensity imbalance, and ρ the total intensity. We work in a regime where the reservoir dynamics adiabatically follows the condensate evolution ($\gamma_R \gg \gamma_c$). Note that both $\phi \in [-\pi, \pi]$, and $z \in [-1, 1]$ are compact variables, while ρ generally increases monotonically with the pump power P . In contrast to most earlier work on synchronization [32], it is crucial to keep track of z and ρ dynamics; amplitude oscillations are pump-dependent and can be large, and dynamics cannot be reduced to a single effective $\dot{\phi}$ equation [?]. Hence, while for two active oscillators a stationary relative phase $\dot{\phi} = 0$ implies their synchronization, here this state persists only if $\dot{z} = \dot{\rho} = 0$ concurrently. However, $\dot{\phi} = 0$ being necessary (though not sufficient) for synchronization can still strongly constrain the synchronized phase.

Generalized Adler Equation - The standard single-variable Adler equation [33] is given by:

$$\dot{\phi} = \Omega - F \sin(\phi) \quad (3)$$

The detuning term Ω causes ϕ to drift linearly in time, while the coupling term $F \sin(\phi)$ encourages the pinning of ϕ to a constant value; the synchronized $\dot{\phi} = 0$ solution is possible only if $-F < \Omega < F$. In the present case, the equation for the relative phase ϕ can be written in a similar form

$$\dot{\phi} = \Omega(z, \rho) - \rho F(\phi, z) \quad (4)$$

In analogy to Eq. (3), we refer to the ϕ -independent term $\Omega(z, \rho)$ as the detuning term (distinct from the pump mode detuning $\Delta\omega_0$), and $\rho F(\phi, z)$ as the coupling term. The ρ dependence of both terms reflects the pump-dependent nature of the nonlinear coupling precipitating the synchronization transition. The condition for $\dot{\phi} = 0$ for the generalized Adler equation becomes:

$$\min_{\phi} \{\rho F(\phi, z)\} < \Omega(z, \rho) < \max_{\phi} \{\rho F(\phi, z)\} \quad (5)$$

where $\max_{\phi}/\min_{\phi}\{f\}$ are the maximum/minimum values respectively taken by $f(\phi, z, \rho)$ as ϕ varies in $[-\pi, \pi]$, for a given (z, ρ) . To understand the implications of this constraint, we study the detuning and coupling terms separately, beginning with the former. In what follows, terms involving mode overlaps (V_{nm} to be introduced, N_{nm}) are purely real, as the trapping potential prevents outgoing flux; in more general cases, a decomposition into real and imaginary parts allows a similar analysis. In the absence of any repulsive interactions, $g, g_R = 0$, the detuning term is simply a constant equal to the pump mode detuning $\Delta\omega_0$, independent of the pump power. This situation becomes more interesting once either type of repulsive interaction is active. If only interactions of polaritons within the condensate are considered - we define this as the

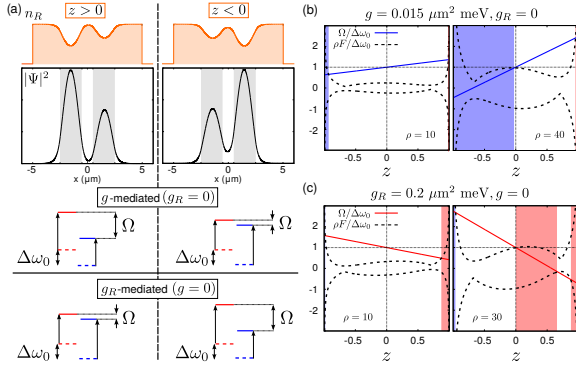


FIG. 2. (a) Schematic variation of detuning term Ω with z in the g -mediated regime (top) and g_R mediated regime (bottom). (b) Evolution of detuning and coupling terms (scaled by $\Delta\omega_0$) with ρ in the g -mediated regime ($g_R = 0$), and (c) the g_R -mediated regime ($g = 0$). Synchronization is not possible in the unshaded regions.

g -mediated regime ($g_R = 0$) - the detuning term in Eq. (4) is modified to:

$$\Omega = (\omega_{l0} + gV_{ll}\bar{a}_l^2 + gV_{lr}\bar{a}_r^2) - (\omega_{r0} + gV_{rr}\bar{a}_r^2 + gV_{rl}\bar{a}_l^2) \quad (6)$$

We have momentarily reverted to amplitude variables \bar{a}_n since each term is intuitively clearest here. The first bracketed term represents the blueshift of the the left trap mode due to repulsion from polaritons occupying that mode ($\propto V_{ll}\bar{a}_l^2$, where $V_{nm} = \int d\mathbf{r} \varphi_n \varphi_m \varphi_m^*$), and from polaritons occupying the right trap mode ($\propto V_{lr}\bar{a}_r^2$); the latter arises since the modes have nonzero spatial overlap. The second line is the corresponding blueshift of the right trap mode. Here $\frac{V_{lr}}{V_{ll}} \approx \frac{V_{rl}}{V_{rr}} \simeq 0.1$, so that the ‘direct’ blueshift is more important and causes the mode with higher occupation to be more strongly blueshifted due to g . The detuning term is thus reduced when the low frequency mode (r) has higher occupation ($\bar{a}_r^2 > \bar{a}_l^2$), namely $z < 0$, and is increased for $z > 0$, as depicted in Fig. 2 (a).

In the g_R -mediated regime where only interactions between reservoir excitons and condensate polaritons are active ($g = 0$), we have instead:

$$\Omega = \left[\omega_l(P) + g_R \frac{\rho\gamma_c}{\gamma_R} N_{ll} \right] - \left[\omega_r(P) + g_R \frac{\rho\gamma_c}{\gamma_R} N_{rr} \right] \quad (7)$$

The exciton repulsion $\propto g_R$ linearly blueshifts the mode frequencies, lending them the P dependence shown in Fig. 1 (c); the homogeneous pump spot ensures an equal blueshift that leaves the pump mode detuning unchanged, $\omega_l(P) - \omega_r(P) = \Delta\omega_0$. However, condensate formation depletes the exciton reservoir population; the reduction in exciton population overlapping with mode n is described by the N_{nn} elements, which are explicitly negative. In this case, the mode with the higher occupation overlaps with a more depleted exciton reservoir, and thus experiences a *weaker* blueshift from the excitons; this is to be contrasted with the g -mediated case where the mode with higher occupation experiences a *stronger* blueshift. The detuning term is thus decreased when the higher frequency

mode (l) has higher occupation, $z > 0$, and increased for $z < 0$, opposite to that in the g -mediated regime [see Fig. 2 (a)]. Note also the additional prefactor of $\gamma_c/\gamma_R = 0.1$ relative to the g -mediated case, which weakens the g_R mediated blueshift.

The coupling term $\rho F(\phi, z)$ does not lend itself as readily to heuristic interpretation as the detuning term. However, our choice of variables immediately indicates that the coupling grows with pump power via the explicit scaling with ρ ; the precise dependence is clarified later. More explicitly, one finds

$$F(\phi, z) \sim g \left[\frac{1}{\sqrt{1-z^2}} \cos \phi + F'_g(2\phi) \right] - N_{12} \left(\frac{\gamma_c}{\gamma_R} \right) \left[\frac{1}{\sqrt{1-z^2}} (R \sin \phi + 2g_R z \cos \phi) + F'_{g_R}(2\phi) \right], \quad (8)$$

a generally complicated function that is periodic in ϕ and diverging as $z \rightarrow \pm 1$; the functions F' contain higher harmonics of ϕ but are non-divergent as functions of z [31]. The coupling may also be divided into a g -mediated and a reservoir mediated term ($\propto N_{rl}$); the latter is again weaker in this regime by the factor γ_c/γ_R , as was the case for the detuning term. Crucially, the strength of the coupling term is approximately unchanged under $z \rightarrow -z$, unlike the detuning term.

Both detuning and coupling terms combine to determine the possibility of a synchronized phase via condition (5). This is best explored graphically, as is done in Fig. 2 (b) for the g -mediated regime; we plot $\max_\phi / \min_\phi \{ \rho F(\phi, z) \}$ (dashed black) and $\Omega(z, \rho)$ (solid blue) for fixed ρ , over the entire range of $z \in [-1, 1]$. The value of ρ is proportional to the pump power: the left panel is for $\rho = 10$, while the right panel shows $\rho = 40$. Condition (5) is satisfied in the shaded regions, and so in the *unshaded* regions, synchronization is impossible; clearly, the $z < 0$ region is preferred here, stemming from the reduced value of Ω in this region. With increasing pump power, the shaded region area grows, as the increasing coupling strength and detuning modification make synchronization easier. The analogous plot in the g_R -mediated regime is shown in Fig. 2 (c), for $\rho = 10$ and $\rho = 30$; the different mechanism for frequency modification manifests in synchronization being preferred here for $z > 0$.

This intuitive description places constraints on $\dot{\phi} = 0$, but does not guarantee synchronization; a complete analysis requires studying the full system of equations given by:

$$\dot{\phi} = 0 = \Delta\omega_0 - \rho G_\phi(\phi, z) \quad (9a)$$

$$\dot{z} = 0 = (\gamma_l - \gamma_r)(1 - z^2) + \rho G_z(\phi, z) \quad (9b)$$

$$\dot{\rho} = 0 = \rho [(\gamma_l + \gamma_r) + (\gamma_l - \gamma_r)z - \rho G_\rho(\phi, z)] \quad (9c)$$

Here we have rewritten the generalized Adler equation [Eq. (4)] to isolate the pump mode detuning. $G_{\phi,z,\rho}$ are functions of system parameters and the variables (ϕ, z) only [31]. While Eqs. (9a)-(9c) cannot be analytically solved for the fixed points, some useful simplifications are possible if both modal gains are taken to be equal, $\gamma_l(P) \approx \gamma_r(P)$ (true in the present case). The $\dot{\rho}$ equation can then be solved to obtain the parametric

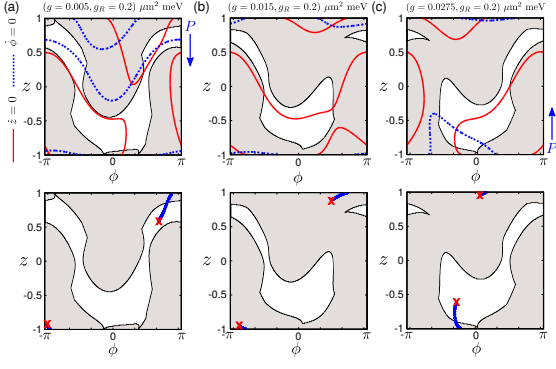


FIG. 3. Top: Stable (plain) and unstable (shaded) regions, with $\dot{z} = 0$ contours (solid red), for (a) g_R -mediated, (c) g -mediated synchronization, and (b) desynchronized regime due to g - g_R competition. Arrows in (a), (c) indicate movement direction of $\phi = 0$ contours. Bottom: Corresponding evolution of fixed points on stability maps for $P \in [1, 1.15]P^L$. Red cross marks final position of a fixed point.

dependence (on ϕ and z) of the fixed points of ρ :

$$\rho_{FP} = \frac{\gamma_l(P) + \gamma_r(P)}{G_\rho(\phi, z)} \quad (10)$$

The only power dependence here comes from the evolution of $\gamma_n(P)$, a quantity that is pre-determined by solving the linear non-Hermitian problem for the pump modes. The function $G_\rho(\phi, z)$ in the denominator is independent of P , and hence for a given set of system parameters and a (ϕ, z) pair, the steady state value of ρ evolves *linearly* with pump power [See Fig. 1(c)]. In what follows, it is then justified to use ρ as a surrogate variable for the pump power P . The \dot{z} equation also simplifies to $\dot{z} = 0 = \rho G_z(\phi, z)$: this implies that for a given set of system parameters, the values of (ϕ, z) for which \dot{z} vanishes are unchanged with increasing ρ , and hence pump power. This simple ρ dependence in fact extends further, to the stability of fixed points as determined by the eigenvalues of the associated Jacobian matrix \mathbf{J} . At the fixed points,

$$\mathbf{J}(\phi, z, \rho)|_{FP} = \rho \begin{pmatrix} -\partial_\phi G_\phi & -\partial_z G_\phi & -\frac{\Delta\omega_0}{\rho^2} \\ \partial_\phi G_z & \partial_z G_z & 0 \\ -\rho\partial_\phi G_\rho & -\rho\partial_z G_\rho & -G_\rho \end{pmatrix} \Big|_{FP} \quad (11)$$

The matrix element $\propto \Delta\omega_0/\rho^2$ is suppressed most strongly by $\rho \propto P$, and can in fact be approximately neglected to lowest order when the synchronization threshold is much larger than the self-oscillation threshold (which is the case here). The Jacobian matrix that remains then has a characteristic equation $\chi(\phi, z, \lambda/\rho) = 0$, which has a crucial implication: the ρ dependence of the characteristic equation serves only to scale its roots, the eigenvalues of the Jacobian matrix [31]. Hence, the *sign* of any eigenvalue does not change as ρ , and therefore pump power, is changed. While this conclusion holds only approximately, and that too at the fixed points of Eqs. (9a)-(9c) at any P , we find that in practice the signs of eigenvalues of \mathbf{J} are quite robust to changes in ρ , for values of ρ close to ρ_{FP} [Eq. (10)] at that pump power.

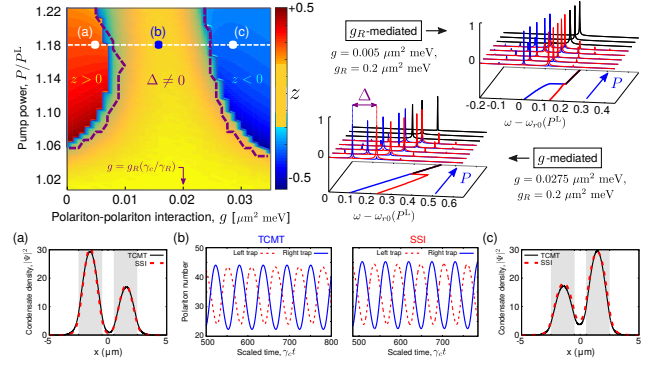


FIG. 4. Phase diagram in P - g space for $g_R = 0.2 \mu\text{m}^2 \text{ meV}$, and evolution with P of typical frequency spectra $\{a_n[\omega]\}$. (a), (c) Steady state $|\Psi|^2$ at correspondingly labelled positions in the two synchronized regions, and comparisons to SSI results. (b) Oscillating polariton number in each trap in the desynchronized regime, computed using the TCMT and SSI.

This simple ρ dependence and the bounded nature of ϕ - z space allows us to introduce meaningfully the concept of a *stability map* for any given set of system parameters: stable regions where all eigenvalues of \mathbf{J} have negative real parts, and unstable regions where at least one such eigenvalue has positive real part, are *unchanged* with pump power. Since ϕ - z space is bounded in $[-\pi, \pi] \times [-1, 1]$, the emergence and movement of fixed points with increasing pump power can be tracked on maps of stable/unstable regions to characterize the global behavior of the system (even though the entire space is not explored for any given initial condition). Since the $\dot{z} = 0$ contours are also unchanged with P , the pump dependence of the generalized Adler equation plays a defining role in the emergence of a synchronized phase with increasing P .

An example of a stability map is shown for the g_R -mediated regime in Fig. 3 (a), with plain regions being stable and shaded regions unstable, and the $\dot{z} = 0$ contours shown in solid red; all of these features are unchanged with pump power. Only the $\dot{\phi} = 0$ contours (dashed blue) change with P ; note that such a contour only exists at points where condition (5) is satisfied. In the g_R -mediated regime, then, it is clear from Fig. 2 (c) that these contours prefer the $z > 0$ region. The trajectories of fixed points with P are shown in the lower panel of Fig. 3 (a). The fixed point in the $z > 0$ region flows with increasing P and enters the stable region; as this crossing occurs, a synchronized phase of the system becomes stable. In the $z < 0$ region, the $\dot{z} = 0$ contour exists in a stable region; however, a stable fixed point cannot emerge until the $\dot{\phi} = 0$ contour spreads in this region, which is clearly restricted based on the analysis leading to Fig. 2 (c). Fig. 3 (c) plots a stability map in the g -mediated regime. Here, the $\dot{\phi} = 0$ contours prefer instead the $z < 0$ region, again clear from Fig. 2 (b). As such, the fixed point that flows from an unstable to a stable region now has $z < 0$, with the $z > 0$ fixed point remaining stationary.

Most interestingly, an intermediate regime exists where the two interactions compete; the different scalings of detuning and

coupling terms discussed earlier imply that for this regime, $g \sim g_R(\gamma_c/\gamma_R)$. A typical stability map here is shown in Fig. 3 (b). For the same range of pump strengths as Fig. 3 (a), (c), the $\dot{\phi} = 0$ contours barely move; this is due simply to the competing effects of g - and g_R -mediated frequency modification, as seen in the generalized Adler equation. As a result, while there are regions where $\dot{z} = 0$ contours exist in stable regions, these are not accessible to the almost static $\dot{\phi} = 0$ contours. Hence, no stable fixed point emerges and a desynchronized phase persists.

These predictions are verified strikingly in a phase diagram obtained via full simulation of the TCMT. As a signature of synchronization, we compute and plot the modal detuning Δ as determined from the Fourier transform of mode coefficients $a_n(t)$ computed once a steady-state is reached. The resulting phase diagram is plotted in the top panel of Fig. 4 in P - g space, at a fixed $g_R = 0.2 \mu\text{m}^2 \text{ meV}$. For small values of $g \ll g_R(\gamma_c/\gamma_R)$ a synchronized phase with a $z > 0$ configuration emerges with increasing pump power. However, with stronger g , a competition arises between the two types of frequency modification effects, preventing synchronization. For values of g that are stronger still, a synchronized phase re-emerges, but now with $z < 0$. Typical frequency spectra in each synchronized region are also included. In dashed purple, we plot the phase boundary as predicted using our analysis of fixed points moving on a fixed stability map computed at $P = 1.15P^L$. The apparent disagreement near the phase boundary simply illustrates the sensitivity of emergent synchronization to initial conditions near this transition. TCMT results are further compared with a direct integration of the full gGPE-reservoir equations [Eqs. (1)] using a standard split-step integrator (SSI); select comparisons are shown in the synchronized regime in Fig. 4 (a), (c), and for the desynchronized regime in Fig. 4 (b), indicating excellent agreement.

We acknowledge helpful discussions with F. Marquardt. This work was supported by the US Department of Energy, Office of Basic Energy Sciences, Division of Materials Sciences and Engineering under Award No. DE-SC0016011.

-
- [1] J Kurths, A Pikovsky, and M Rosenblum. *Synchronization: A Universal Concept in Nonlinear Sciences*. Cambridge University Press, Cambridge, England, 2001.
 - [2] Matthew H. Matheny, Matt Grau, Luis G. Villanueva, Rassul B. Karabalin, M.C. Cross, and Michael L. Roukes. Phase Synchronization of Two Anharmonic Nanomechanical Oscillators. *Physical Review Letters*, 112(1):014101, January 2014.
 - [3] Mian Zhang, Gustavo S. Wiederhecker, Sasikanth Manipatruni, Arthur Barnard, Paul McEuen, and Michal Lipson. Synchronization of Micromechanical Oscillators Using Light. *Physical Review Letters*, 109(23):233906, December 2012.
 - [4] C. A. Holmes, C. P. Meaney, and G. J. Milburn. Synchronization of many nanomechanical resonators coupled via a common cavity field. *Physical Review E*, 85(6):066203, June 2012.
 - [5] Mahmood Bagheri, Menno Poot, Linran Fan, Florian Marquardt, and Hong X. Tang. Photonic Cavity Synchronization of Nanomechanical Oscillators. *Physical Review Letters*, 111(21):213902, November 2013.
 - [6] H.-J. Wünsche, S. Bauer, J. Kreissl, O. Ushakov, N. Korneyev, F. Henneberger, E. Wille, H. Erzgräber, M. Peil, W. Elsässer, and I. Fischer. Synchronization of Delay-Coupled Oscillators: A Study of Semiconductor Lasers. *Physical Review Letters*, 94(16):163901, April 2005.
 - [7] O. Malik, K. G. Makris, and H. E. Türeci. Spectral method for efficient computation of time-dependent phenomena in complex lasers. *Physical Review A*, 92(6):063829, December 2015.
 - [8] Fabian Böhm, Anna Zakharova, Eckehard Schöll, and Kathy Lüdge. Amplitude-phase coupling drives chimera states in globally coupled laser networks. *Physical Review E*, 91(4):040901, April 2015.
 - [9] Michael R. Hush, Weibin Li, Sam Genway, Igor Lesanovsky, and Andrew D. Armour. Spin correlations as a probe of quantum synchronization in trapped-ion phonon lasers. *Physical Review A*, 91(6):061401, June 2015.
 - [10] Tony E. Lee and H. R. Sadeghpour. Quantum Synchronization of Quantum van der Pol Oscillators with Trapped Ions. *Physical Review Letters*, 111(23):234101, December 2013.
 - [11] Minghui Xu, D.A. Tieri, E.C. Fine, James K. Thompson, and M.J. Holland. Synchronization of Two Ensembles of Atoms. *Physical Review Letters*, 113(15):154101, October 2014.
 - [12] A. B. Cawthorne, P. Barbara, S. V. Shitov, C. J. Lobb, K. Wiesenfeld, and A. Zangwill. Synchronized oscillations in Josephson junction arrays: The role of distributed coupling. *Physical Review B*, 60(10):7575–7578, September 1999.
 - [13] M. C. Cross, A. Zumdick, Ron Lifshitz, and J. L. Rogers. Synchronization by Nonlinear Frequency Pulling. *Physical Review Letters*, 93(22):224101, November 2004.
 - [14] Georg Heinrich, Max Ludwig, Jiang Qian, Björn Kubala, and Florian Marquardt. Collective Dynamics in Optomechanical Arrays. *Physical Review Letters*, 107(4):043603, July 2011.
 - [15] A. Mari, A. Farace, N. Didier, V. Giovannetti, and R. Fazio. Measures of Quantum Synchronization in Continuous Variable Systems. *Physical Review Letters*, 111(10):103605, September 2013.
 - [16] Max Ludwig and Florian Marquardt. Quantum Many-Body Dynamics in Optomechanical Arrays. *Physical Review Letters*, 111(7):073603, August 2013.
 - [17] Tony E. Lee, Ching-Kit Chan, and Shenshen Wang. Entanglement tongue and quantum synchronization of disordered oscillators. *Physical Review E*, 89(2):022913, February 2014.
 - [18] Niels Lörch, Ehud Amitai, Andreas Nunnenkamp, and Christoph Bruder. Genuine Quantum Signatures in Synchronization of Anharmonic Self-Oscillators. *Physical Review Letters*, 117(7):073601, August 2016.
 - [19] Michiel Wouters. Synchronized and desynchronized phases of coupled nonequilibrium exciton-polariton condensates. *Physical Review B*, 77(12):121302, March 2008.
 - [20] A. Baas, K. G. Lagoudakis, M. Richard, R. André, Le Si Dang, and B. Deveaud-Plédran. Synchronized and Desynchronized Phases of Exciton-Polariton Condensates in the Presence of Disorder. *Physical Review Letters*, 100(17):170401, April 2008.
 - [21] P. R. Eastham. Mode locking and mode competition in a nonequilibrium solid-state condensate. *Physical Review B*, 78(3):035319, July 2008.
 - [22] L. A. Lugiato, L. M. Narducci, and C. Oldano. Cooperative frequency locking and stationary spatial structures in lasers. *Journal of the Optical Society of America B*, 5(5):879, May 1988.
 - [23] Chr. Tamm. Frequency locking of two transverse optical modes of a laser. *Physical Review A*, 38(11):5960–5963, December 1988.

- [24] D. Y. Tang, R. Dykstra, and N. R. Heckenberg. Synchronization of chaotic laser mode dynamics. Physical Review A, 54(6):5317–5322, December 1996.
- [25] M. Bennett, M. F. Schatz, H. Rockwood, and K. Wiesenfeld. Huygens’s clocks. Proceedings of the Royal Society A: Mathematical, Physical and Engineering Sciences, 458(2019):563–579, March 2002.
- [26] Ch Huygens. Horologium Oscillatorium. Apud F. Muguet, Paris, France, 1673.
- [27] Hakan E. Türeci and A. Douglas Stone. Mode competition and output power in regular and chaotic dielectric cavity lasers. page 255, April 2005.
- [28] Saeed Khan and Hakan E. Türeci. Non-Hermitian coupled-mode theory for incoherently pumped exciton-polariton condensates. arXiv:1608.07557 [cond-mat], August 2016. arXiv:1608.07557.
- [29] M. Abbarchi, A. Amo, V. G. Sala, D. D. Solnyshkov, H. Flayac, L. Ferrier, I. Sagnes, E. Galopin, A. Lemaître, G. Malpuech, and J. Bloch. Macroscopic quantum self-trapping and Josephson oscillations of exciton polaritons. Nature Physics, 9(5):275–279, May 2013.
- [30] F. Baboux, L. Ge, T. Jacqmin, M. Biondi, E. Galopin, A. Lemaître, L. Le Gratiet, I. Sagnes, S. Schmidt, H.E. Türeci, A. Amo, and J. Bloch. Bosonic Condensation and Disorder-Induced Localization in a Flat Band. Physical Review Letters, 116(6):066402, February 2016.
- [31] See Supplemental Material at ‘URL’ for derivation of the TCMT, complete expressions for equations, typical system dynamics, and Jacobian matrix analysis.
- [32] Juan A. Acebrón, L. L. Bonilla, Conrad J. Pérez Vicente, Flix Ritort, and Renato Spigler. The Kuramoto model: A simple paradigm for synchronization phenomena. Reviews of Modern Physics, 77(1):137–185, April 2005.
- [33] R. Adler. A Study of Locking Phenomena in Oscillators. Proceedings of the IRE, 34(6):351–357, June 1946.